# Atypical Teratoid/Rhabdoid Tumor

Adekunle M. Adesina, Jill V. Hunter,
and Lucy Balian Rorke-Adams

## 9.1 Overview

- Atypical teratoid/rhabdoid tumors (AT/RTs) are malignant, high-grade embryonal (WHO Grade IV) tumors seen in children often below the age of 3 years and rarely above the age of 6 years.
- AT/RTs account for 10 % of tumors in infants, with a male:female ratio of 2:1.
- They are characteristically poorly differentiated, contain rhabdoid cells with divergent differentiation to form epithelial, mesenchymal, neuronal, and glial components, and may be associated with a subpopulation of primitive neuroectodermal cells.

## 9.2 Clinical Features

- Presenting symptoms are related to location, which may include the cerebral hemispheres; suprasellar, pineal, or cerebellar sites; the cerebellopontine angle (CPA); or rarely, the spinal cord.
- Symptoms of raised intracranial pressure, including vomiting and lethargy, may occur.
- Cranial nerve palsy may be seen in CPA and brainstem lesions.
- Leptomeningeal dissemination is frequent and may be a presenting feature in a significant subset.
- An aggressive clinical course is typical.

A.M. Adesina, M.D., Ph.D. (✉)
Department of Pathology, Texas Children's Hospital,
Baylor College of Medicine, One Baylor Plaza, RM 286A,
Houston, TX 77030, USA
e-mail: aadesina@bcm.tmc.edu

J.V. Hunter, M.B.B.S.
Department of Radiology, Texas Children's Hospital,
6621 Fannin Street, Houston, TX 77030, USA

L.B. Rorke-Adams, M.D.
Department of Pathology, The Children's Hospital of Philadelphia,
34th Street and Civic Center Boulevard, Philadelphia, PA 19104, USA

## 9.3 Neuroimaging

- The tumor may present as a supratentorial mass (Figs. 9.1 and 9.2) or, more commonly, an infratentorial mass (Fig. 9.3), classically involving the CPA (Figs. 9.4, 9.5, 9.6, and 9.7).
- Though uncommon, it may also present as a spinal cord mass lesion (Fig. 9.8).
- Characteristically, MRI shows a predominantly solid mass that is hyperintense or isointense with gray matter, with moderate diffuse heterogeneous enhancement (Figs. 9.1, 9.2, and 9.9).
- Cystic areas and regions of necrosis may be present (Fig. 9.10A).
- There is typically associated restricted diffusion (Figs. 9.10B and 9.11) consistent with a densely cellular tumor. The neuroimaging appearance can be radiographically indistinguishable from medulloblastoma.
- MR spectroscopy shows marked elevation of the choline peak, with little, if any, N-acetylaspartate (NAA) peak.
  - There may be an associated lipid/lactate peak within the tumor, consistent with tumor necrosis.
- Diffuse leptomeningeal enhancement within the brain and spine is frequent; when present, it is consistent with cerebrospinal fluid (CSF) dissemination.

## 9.4 Pathology

- *Gross pathology*
  - Grossly, tumors are variably sized, soft, and variegated, with pink-red hemorrhagic and sometimes necrotic appearance. In contrast to primitive neuroectodermal tumor (PNET), they more often contain foci of necrosis and hemorrhage.
  - A significant mesenchymal component may confer a firm consistency. Uncommonly, they may contain small, dense, white foci reflecting a connective tissue component.

**Fig. 9.1** Axial T1-weighted MR image (**A**) and T2-weighted image (**B**) in a 16-month-old boy, demonstrating a solid-appearing, heterogeneous mass occupying most of the body of the left lateral ventricle with bowing of the midline convex to the right in the presence of a dilated supratentorial ventricular system
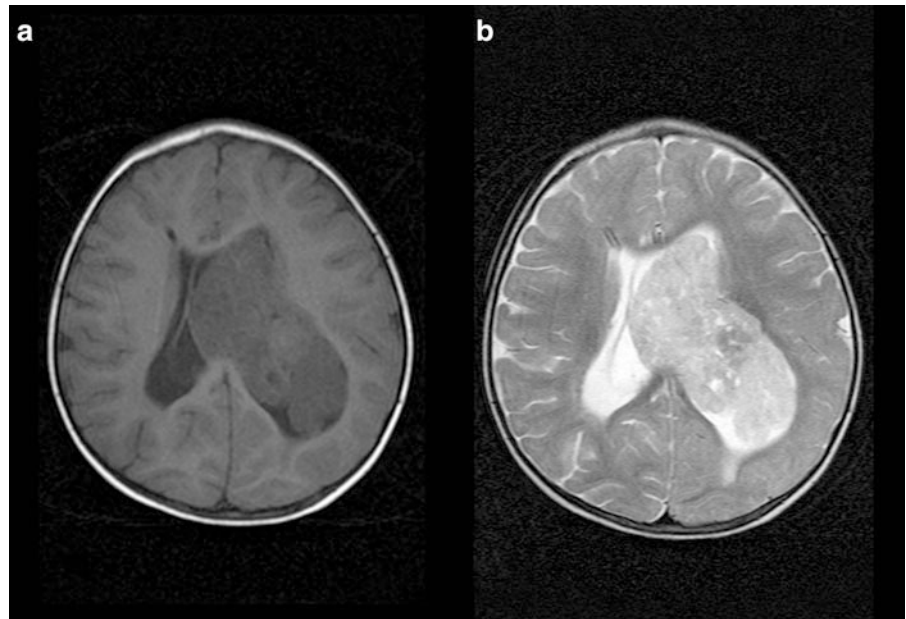


**Fig. 9.2** Axial T2-weighted image (**A**) and T1-weighted image (**B**) after gadolinium enhancement in a 22-month-old girl, demonstrating a rim-enhancing, mixed solid and cystic-appearing supratentorial tumor effacing the body of the right lateral ventricle and causing contralateral hydrocephalus with transependymal fluid spread on the left. Histopathology revealed an atypical teratoid/rhabdoid tumor (AT/RT). Following a gross total resection and therapy, this child survived for another 5 years
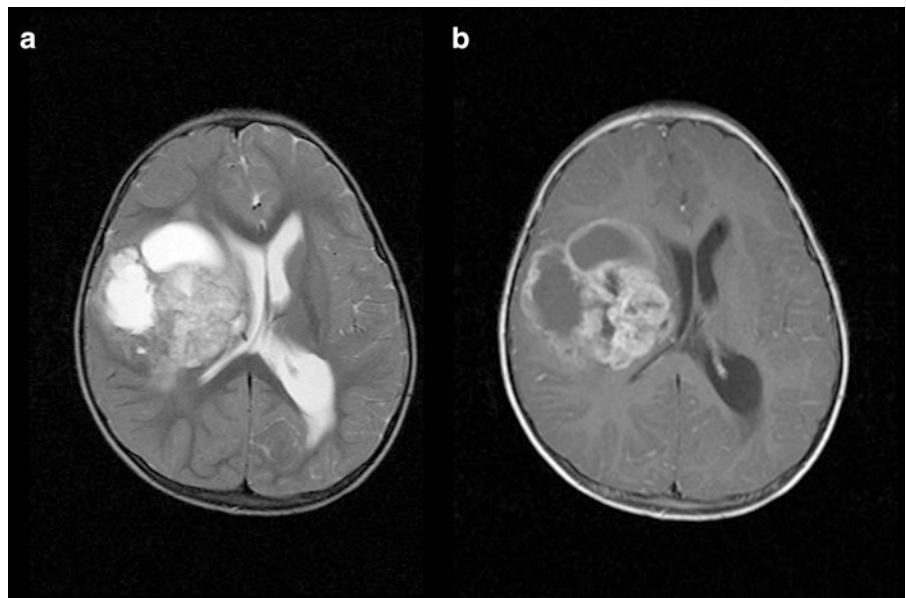


- *Intraoperative smears*
  - Cytologic preparations are often cellular, with cells arranged in predominantly cohesive clusters in a necrotic background showing tumor diathesis. Rare or occasional pseudopapillary configuration (Fig. 9.12A) may be seen.
  - The cells are poorly differentiated, often epithelioid, and may consist of a variable component of typical rhabdoid cells with moderate size, pink cytoplasm, and a round, eccentrically placed nucleus having a prominent nucleolus (Fig. 9.12B inset).
  - Poorly differentiated cells with hyperchromatic nuclei and little cytoplasm (reminiscent of the "small blue cells" of a PNET) may be present (Fig. 9.12B).
  - Frequent mitosis, apoptosis, and cell wrapping can be seen.
- *Histology*
  - Histology is variable and complex. It may show solely sheets of rhabdoid cells (Fig. 9.13), or may consist primarily of primitive neuroectodermal cells (Fig. 9.14).
  - Lesions tend to be necrotic and hemorrhagic, and may contain foci of dystrophic calcification. Dilated, thrombosed blood vessels are sometimes seen as well.
  - Rhabdoid cells are poorly differentiated, with eccentric vesicular nuclei, prominent nucleoli, and eosinophilic (ground glass) cytoplasm containing distinct globular inclusions and with distinct cell borders (Fig. 9.15).

**Fig. 9.3** Axial T2-weighted image through the posterior fossa in a 21-month-old boy, demonstrating heterogeneous, mixed signal-intensity mass with solid and more cystic-appearing components extending into the left cerebellopontine angle (CPA), with nonvisualization of the fourth ventricle



**Fig. 9.4** Unenhanced CT examination in an 18-month-old boy who presented with hearing loss, showing a hyperdense mass originating at the level of the left CPA. The hyperdensity suggests a highly cellular tumor, confirmed on MRI with restricted-diffusion abnormality in the presence of altered blood and blood product. Bone windows on CT revealed some remodeling of the left internal auditory canal (IAC), in the presence of an otitis media. Despite resection that revealed an AT/RT, the child died 1 month later

- ○ Disparate tissues or cells, which are often recognizable without too much difficulty, may include spindled mesenchymal-type cells (Fig. 9.16A) or rare epithelium, which may be squamous (Fig. 9.16B) and/or adenomatous (Fig. 9.16C).
- ○ Regional epithelial differentiation showing a papillary, adenomatous, or cordlike pattern (Fig. 9.17) may be seen. More commonly, evidence of epithelial differentiation is perceived only by antigen expression.
- ○ Regions of cells with prominent cytoplasmic vacuolization are frequent and should raise the differential diagnosis of AT/RT (Fig. 9.18).
- ○ Mesenchymal differentiation with a desmoplastic spindle cell pattern or frank sarcomatous differentiation may be seen (Fig. 9.19).
- ○ Mitotic activity is high, atypical mitoses can be readily identified, and cell wrapping may be seen.
- ○ A regional component of primitive neuroectodermal cells is frequently seen, but their presence is not required to reach a diagnosis of AT/RT. The fields of primitive neuroepithelial cells generally resembling the so-called classic medulloblastoma, which may exhibit Homer Wright rosettes, is seen in 60–70 % of AT/RTs.
- ○ Rarely, a classic neurotubular structure characteristic of medulloepithelioma is encountered.
- ○ The nodular architecture characteristic of desmoplastic or "neuroblastic" medulloblastoma is not found in AT/RTs, but distinguishing AT/RT from anaplastic and large cell medulloblastoma is challenging.
- ○ Tumors that occur in more than one site may exhibit histologic features that differ. For example, one may be composed entirely of rhabdoid cells, whereas another may be indistinguishable from a PNET/medulloblastoma (PNET/MB).

## 9.5    Immunohistochemistry

- The rhabdoid cells typically show immunopositivity for epithelial membrane antigen (EMA) (Fig. 9.20A) and vimentin (Fig. 9.20B), with variable expression of smooth muscle actin (SMA) (Fig. 9.20C).
- Focal or regional positivity for cytokeratin (Fig. 9.20D), glial fibrillary acidic protein (GFAP) (Fig. 9.20E), and neuronal markers such as synaptophysin (Fig. 9.20F) and neurofilament proteins (NFP) (Fig. 9.20G) may be seen.
- Immunostaining for SMARCB1/INI1 protein is negative in tumor cell nuclei but present in endothelial cell nuclei, which serve as an internal control (Fig. 9.20H).
  - ○ Lack of expression of the INI1 antigen is most helpful in differentiating AT/RT from look-alikes and is an indication of the rhabdoid nature of the cells.
- Ki-67 shows a high proliferation index, often ranging between 25 % and 85 %.

**Fig. 9.5** (**A**) Axial T2-weighted image demonstrating a right CPA mass. (**B**) Restricted diffusion abnormality on an apparent diffusion coefficient (ADC) map
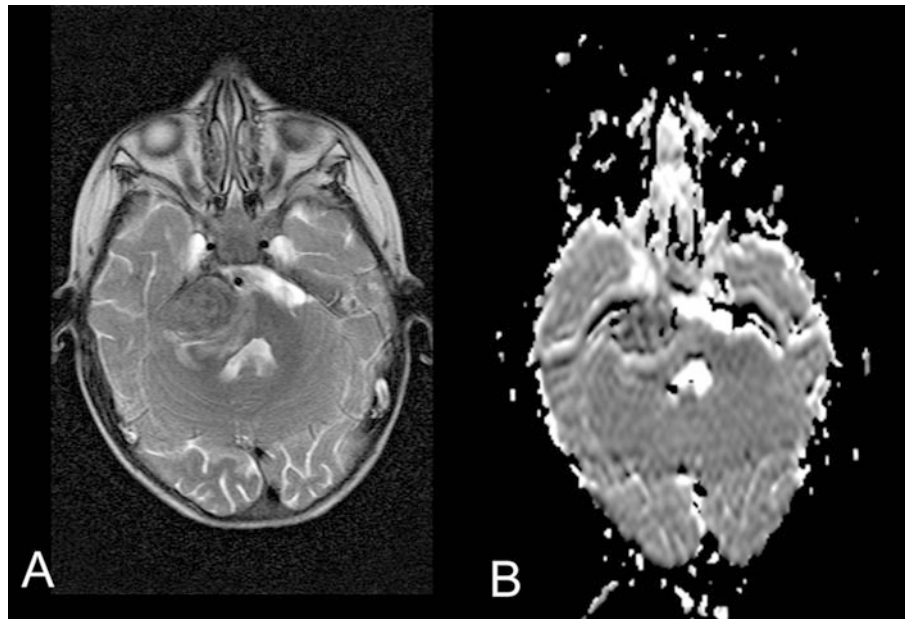


**Fig. 9.6** Evidence for hemorrhage within the tumor on gradient echo imaging (**A**) in the same patient as Fig. 9.5. Fine cut, heavily T2-weighted imaging (**B**) demonstrates exophytic extension into the basal cistern
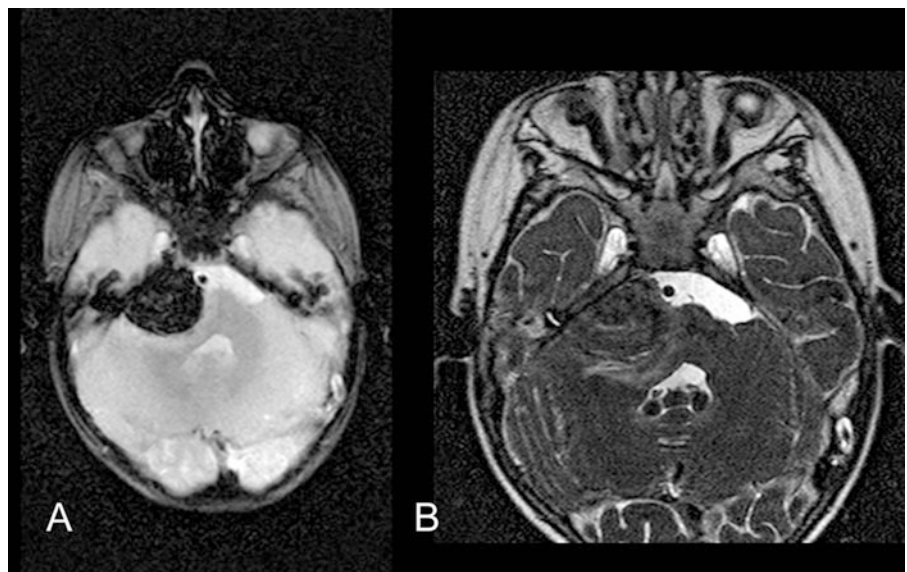


**Fig. 9.7** (**A**, **B**) Fine cut, T1-weighted imaging of the same patient as Fig. 9.5 shows the pattern of enhancement, which extends into the porus of the right IAC. The patient survived for another 6 months despite resection and therapy
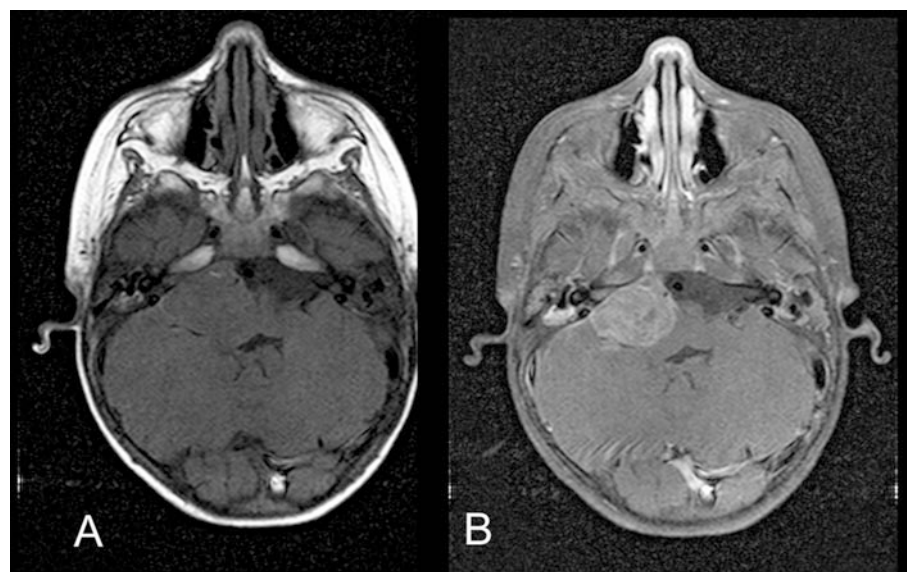
**Fig. 9.8** Sagittal T1-weighted imaging of the head (**A**) and neck (**B**) of a 1-year-old girl who presented with left-sided weakness, before and after the administration of gadolinium, showing an extradural mass lesion in the cervical spine with post-Gd rim enhancement. This lesion proved to be a rhabdoid tumor with extension through the exit foramen into the soft tissues, requiring more than one resection. This is a very unusual location for AT/RT. The patient died from intracranial dissemination of tumor 4 months after first presentation
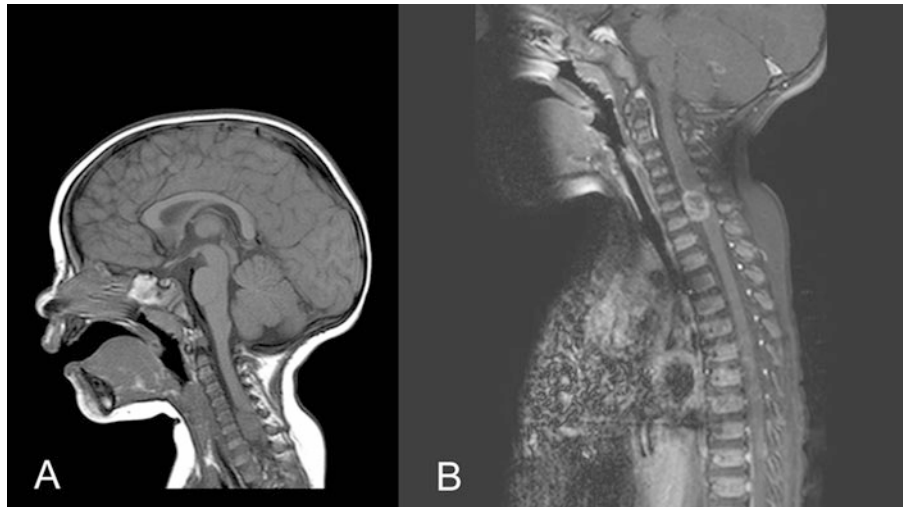


**Fig. 9.9** Axial T2-weighted (**A**) and T1-weighted (**B**) post-Gd images of a 17-month-old boy with a large, poorly enhancing, predominantly hyperintense lesion in the left frontal region, causing mass effect and midline shift with contralateral hydrocephalus. The lesion proved to be a supratentorial AT/RT. The patient survived for 5 months following removal
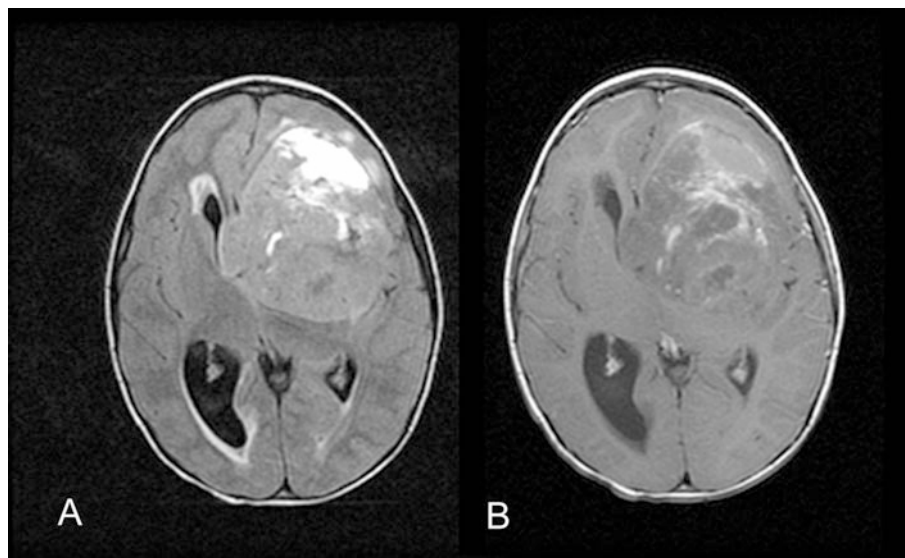


**Fig. 9.10** Axial T1-weighted post-Gd imaging (**A**) and axial diffusion-weighted imaging (DWI) (**B**) in the same patient as in Fig. 9.3, demonstrating diffuse enhancement of the solid-appearing component of the tumor, which shows restricted diffusion abnormality on an ADC map. The right posterior component of the tumor demonstrates unrestricted diffusion consistent with a fluid-filled cyst. Taking the morphology into account, these appearances would be typical for an AT/RT, but differential diagnosis would include medulloblastoma and anaplastic ependymoma. This patient survived for another 5 years with treatment
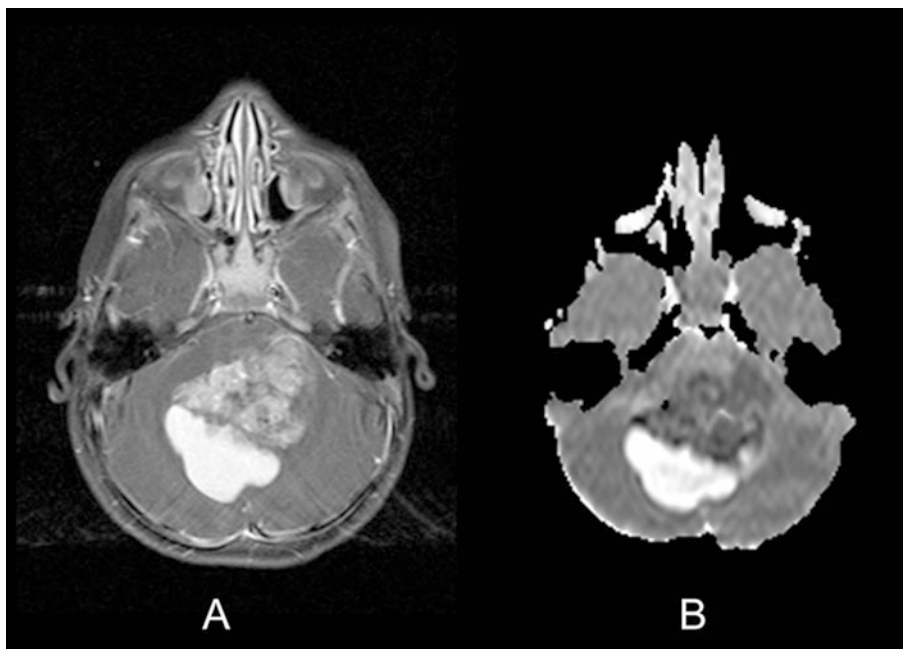
**Fig. 9.11** Axial ADC map (**A**) and T1-weighted post-Gd imaging (**B**) in the same patient as in Fig. 9.5, demonstrating almost uniformly restricted diffusion abnormality in the poorly enhancing intraventricular mass, which at surgery proved to be a supratentorial AT/RT. Despite a gross total resection, this patient survived only 2 months
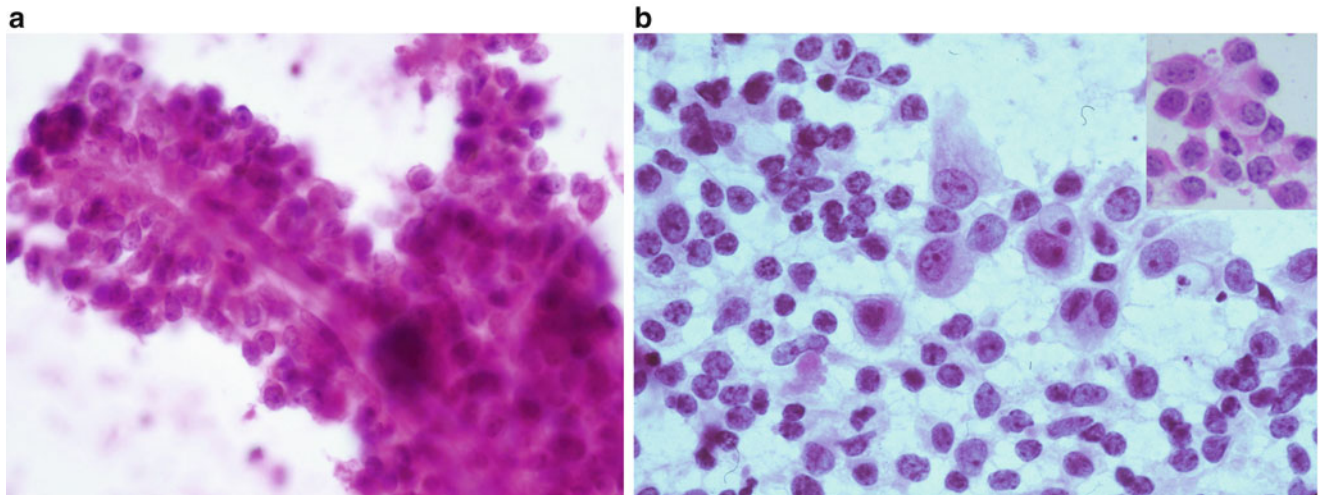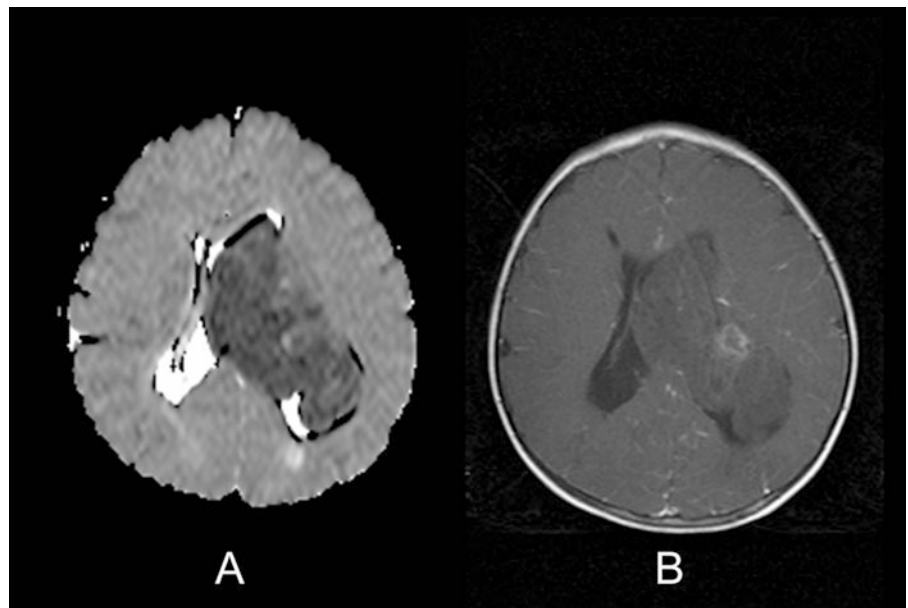


**Fig. 9.12** Intraoperative cytologic preparations showing malignant, poorly differentiated tumor cells arranged in a pseudopapillary pattern (**A**); A smear of a rhabdoid tumor (**B**) with a mixed population of primitive neuroepithelial cells and rhabdoid cells (H&E, ×600). The *inset* shows rhabdoid cells with vesicular nuclei and prominent nucleoli
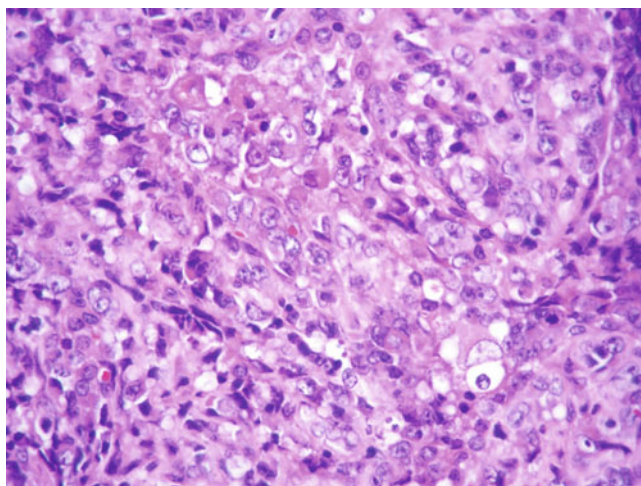
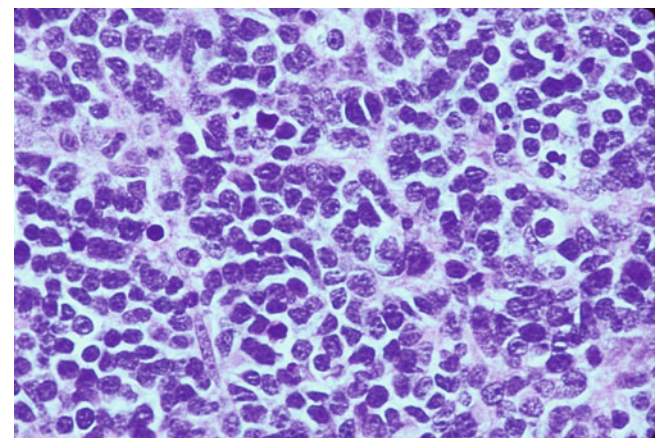**Fig. 9.13** Histology of AT/RT showing sheets of epithelioid cells

**Fig. 9.14** Region in an AT/RT showing poorly differentiated, primitive neuroepithelial cells or "small blue cells" consistent with an embryonal neuroepithelial (PNET-like) component (H&E, ×400)
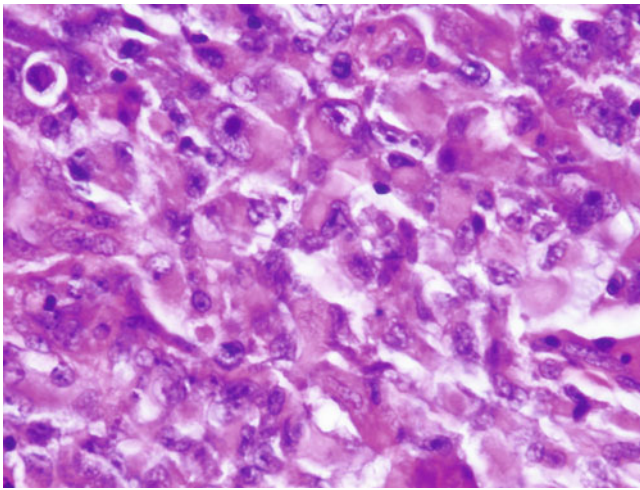
**Fig. 9.15** Epithelioid (rhabdoid) cells with vesicular nuclei, prominent nucleoli, and abundant, eccentric, eosinophilic cytoplasm

## 9.6 Electron Microscopy

- The characteristic ultrastructural feature of rhabdoid cells is the presence of whorls of intermediate filaments in the perikaryon (Figs. 9.21A and B).
- Undifferentiated neuroepithelial cells have a small cell body, most of which is occupied by the nucleus, with only a few organelles.
- Differentiated neuroepithelial cells show intermediate filaments, microtubules, and/or dense core vesicles.
- Epithelial cells exhibit desmosomes or longer junctions similar to zonulae adherentes, cilia, or other specific features of epithelial differentiation (Fig. 9.21C).
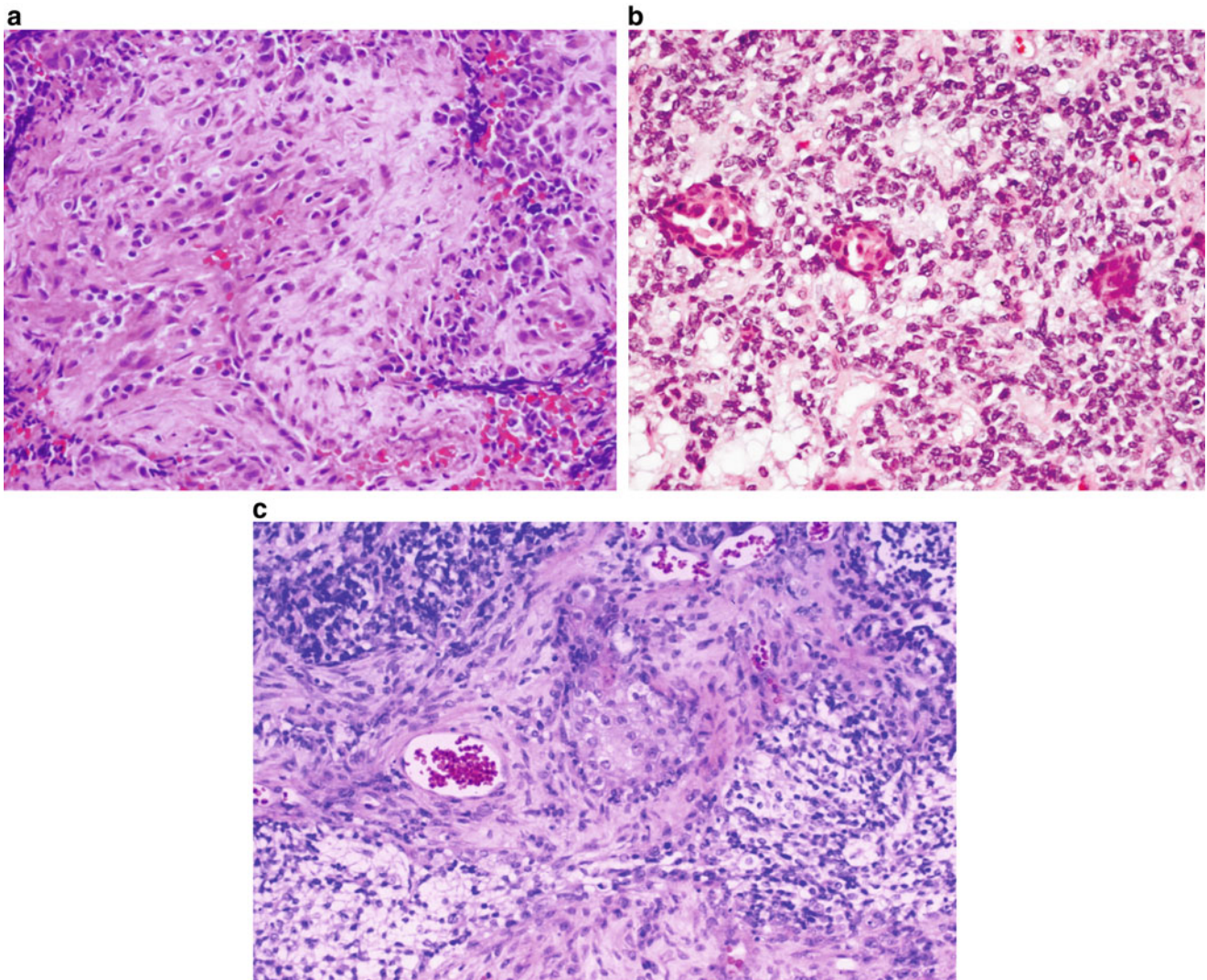


**Fig. 9.16** Regional desmoplasia is a common finding in AT/RT with tissue culture type fibroblastic proliferation (**A**), abrupt nests of squamous differentiation (**B**), and field of AT/RT containing a nest of squamous and glandular epithelium in the center (**C**), with a small amount of surrounding nondifferentiating, collagenous mesenchymal tissue and nests of primitive epithelial cells (*upper left* and *lower right*) (H&E, ×100)
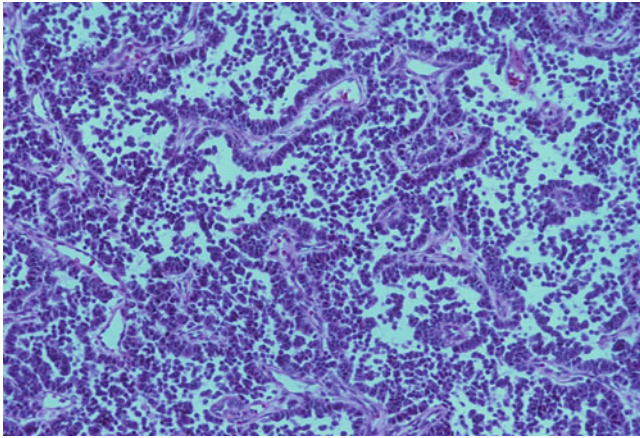
**Fig. 9.17** Field of AT/RT composed of papillary structures and primitive neuroepithelial cells (H&E, ×100)
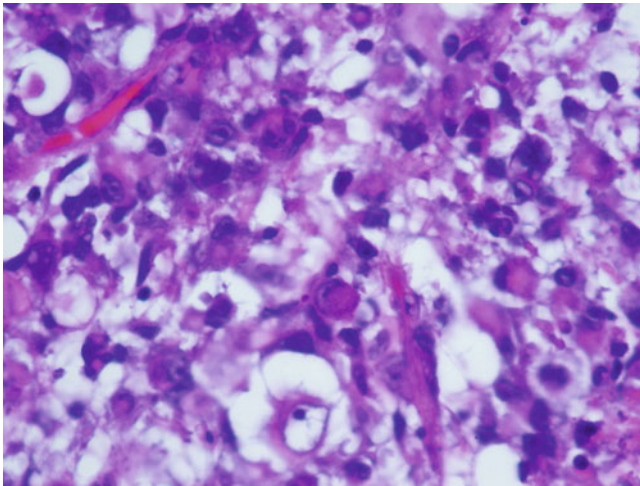


**Fig. 9.18** Regional cytoplasmic vacuolization is common and may involve large regions of an AT/RT (H&E, ×400)
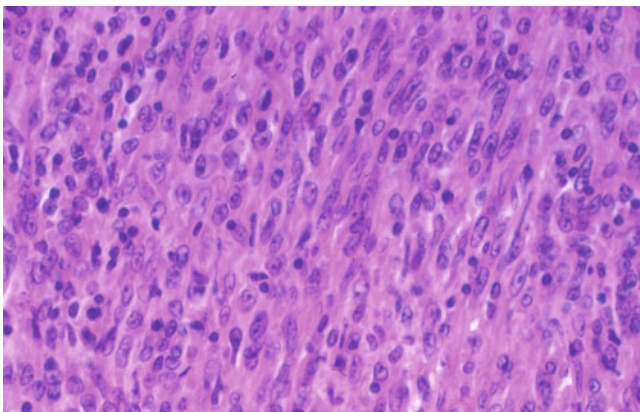


**Fig. 9.19** Field consisting of elongated spindled cells resembling a sarcoma (H&E, ×250)

## 9.7 Differential Diagnosis

- Major differential diagnoses include the classic type of PNET/MB, anaplastic and large cell medulloblastoma, and choroid plexus carcinoma.
- The divergent histologic features and immunophenotype often raise the possibility of a germ cell tumor, but the absence of differentiation into elements of the three germ layers can be helpful in distinguishing AT/RTs from germ cell tumors.
- AT/RTs do not express desmin or germ cell markers such as alpha-fetoprotein (AFP) and beta human chorionic gonadotropin (β-hCG).
- Regions of cells with prominent cytoplasmic vacuolization may be a shared histologic feature with choroid plexus carcinoma and may be problematic with small biopsies, but choroid plexus carcinoma shows nuclear positivity for INI1 protein.
- Interpretation of immunohistochemical findings may be complicated by the fact that PNET areas may express GFAP, NFP, vimentin, SMA, and, rarely, desmin. However, the primitive-appearing cells do not express EMA or keratin.
- Biopsies with PNET-like features and negative nuclear staining for INI1 should be regarded as representing a PNET-like region of an AT/RT.
- The neoplastic mesenchymal component in AT/RT may resemble a sarcoma. If this pattern predominates, it poses a major risk of misdiagnosis.
- Tumors that occur in more than one site may exhibit histological features that differ. For example, one may be composed entirely of rhabdoid cells, whereas another may be indistinguishable from a PNET/MB.
- Anaplastic or large cell medulloblastoma may mimic AT/RT but can be easily differentiated by nuclear positivity for INI1.
- Rhabdoid meningioma shares the rhabdoid morphology with AT/RT, but unlike AT/RT, it usually shows immunopositivity for INI1.

## 9.8 Molecular Pathology

- A characteristic genetic event seen in 85 % of AT/RTs involves the deletion of the *SMARCB1/INI1* (*hSNF5*) locus at 22q11.2 and/or mutation of the *INI* gene (Fig. 9.20I).
- Biallelic (homozygous) deletion (Fig. 9.20J) or mutation of one allele followed by the loss of the second allele during homologous recombination represents a mechanism of inactivation of INI1 expression.
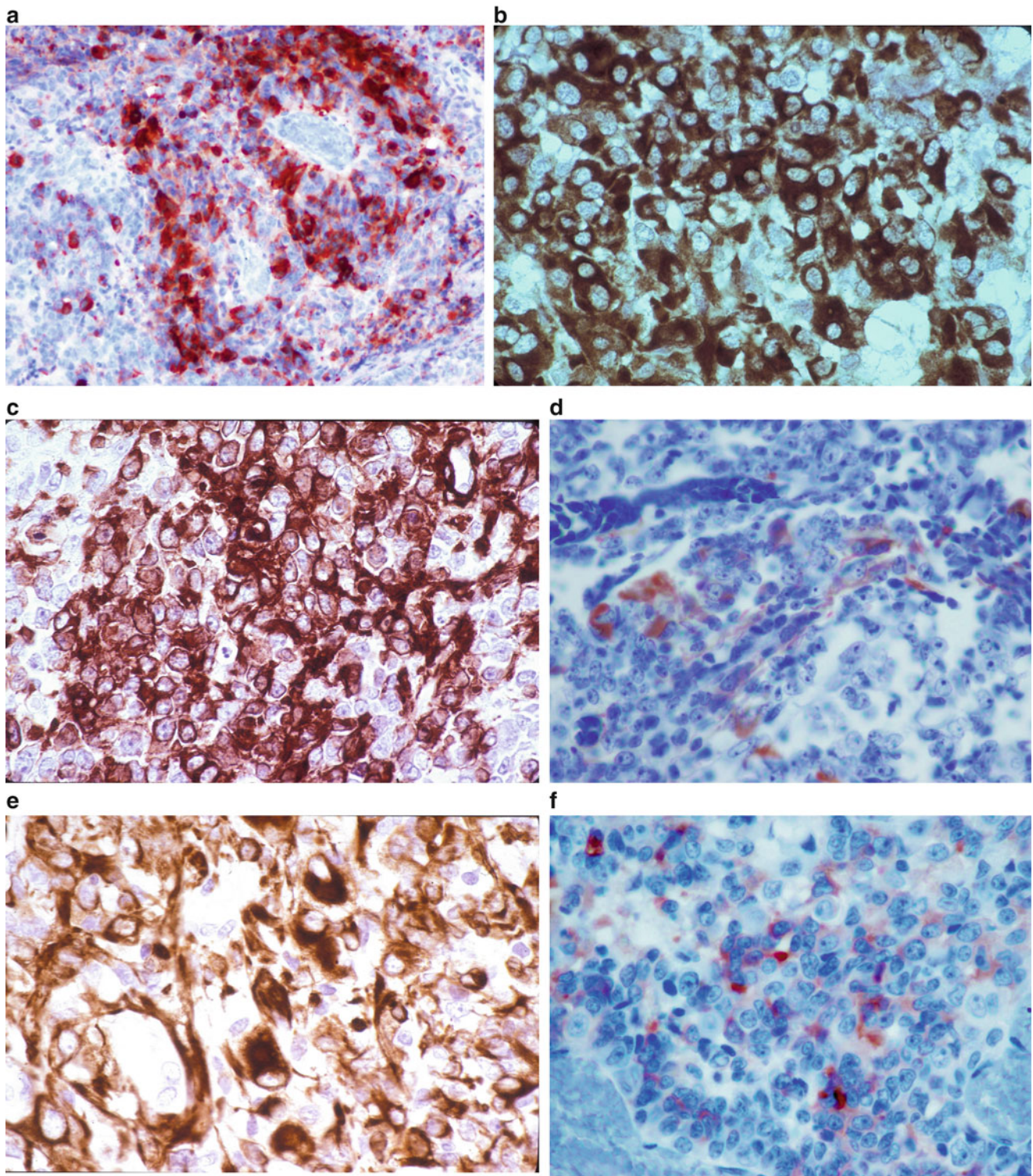
**Fig. 9.20** Photomicrographs of AT/RT demonstrating expression of various antigens: (**A**) Epithelial membrane antigen (EMA) (×400). (**B**) Vimentin (×400). (**C**) Smooth muscle actin (SMA) (×400). (**D**) AE1/ AE3 pan-cytokeratin (keratin) (×400). (**E**) Glial fibrillary acidic protein (GFAP) (×250). (**F**) Synaptophysin (×400). (**G**) Neurofilament proteins (NFP) (×250). (**H**) INI1 (×400). Note positive immunostaining of the nuclei of endothelial cells and negative staining in tumor cells. (**I, J**) Fluorescence in situ hybridization (FISH) analysis of AT/RT shows heterozygous (allelic) deletion at the SMARCB1/INI1 (hSNF5) locus at 22q11.2 (**I**), with the ratio of the test probe (*green*) to the reference probe (*red*) ratio less than 0.8, and homozygous (biallelic) deletion at the SMARCB1/INI1 (hSNF5) locus at 22q11.2 (**J**). In this image, the test probe is *red*; the reference probe is *green*
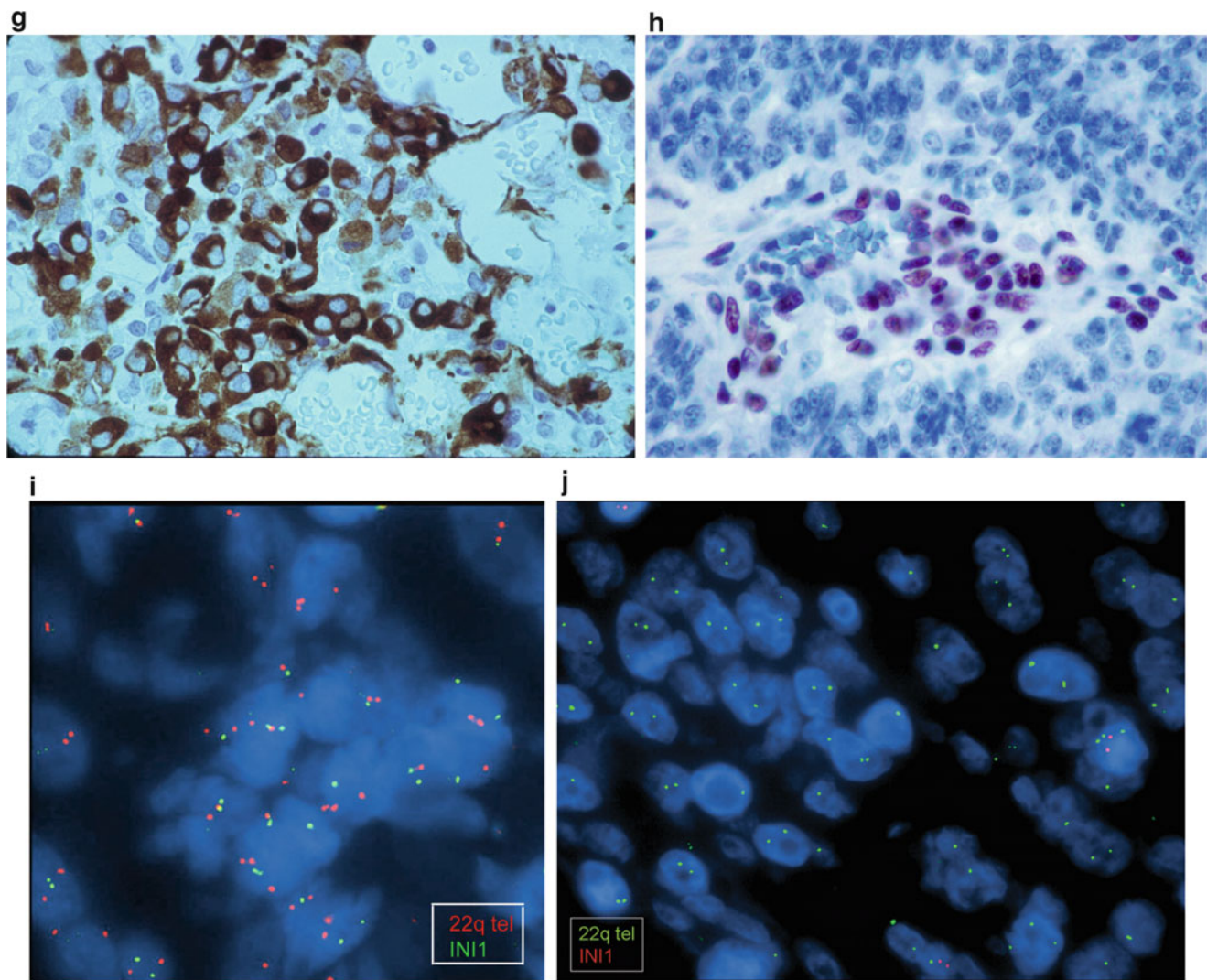
**Fig. 9.20** (continued)

- Most of the mutations are nonsense or frameshift mutations leading to loss of expression of the INI1 protein.
- Loss of expression of INI1 protein without demonstrable gene mutation or hypermethylation of the *INI1* gene promoter region has been described.
- Germline mutations involving the *SMARCB1/hSNF5/INI1* gene are associated with a novel autosomal dominant syndrome, the rhabdoid predisposition syndrome (RPS), with incomplete penetrance that predisposes to malignant posterior fossa brain tumors in infancy. Some of these cases represent recurrent, interstitial deletions mediated by low copy repeats in 22q11.2, with a predisposition to cancer.
- The spectrum of neoplasia that may be seen in RPS includes CNS AT/RTs, central PNETs, medulloblastoma, and choroid plexus carcinoma, as well as rhabdoid tumors in the kidneys and extrarenal tissues.

- The mechanism of action of the wild-type INI protein in the prevention of neoplastic transformation is unclear.
- Nonsense mutation and inactivation of *SMARCA4* (*BRG1*) has been reported in a rare subset of AT/RTs showing no mutation of *SMARCB1* and with retained nuclear expression of INI1 protein.
- SMARCA4 is a subunit of several different SWI/SNF protein complexes. It enhances Notch-dependent proliferative signals, thereby promoting neural stem cell self-renewal and proliferation while concurrently making the neural stem cell insensitive to *SHH*-dependent differentiating cues.

## 9.9 Prognosis

- Outcome in children less than 3 years of age is poor, with survival ranging between 11 months and 24 months.
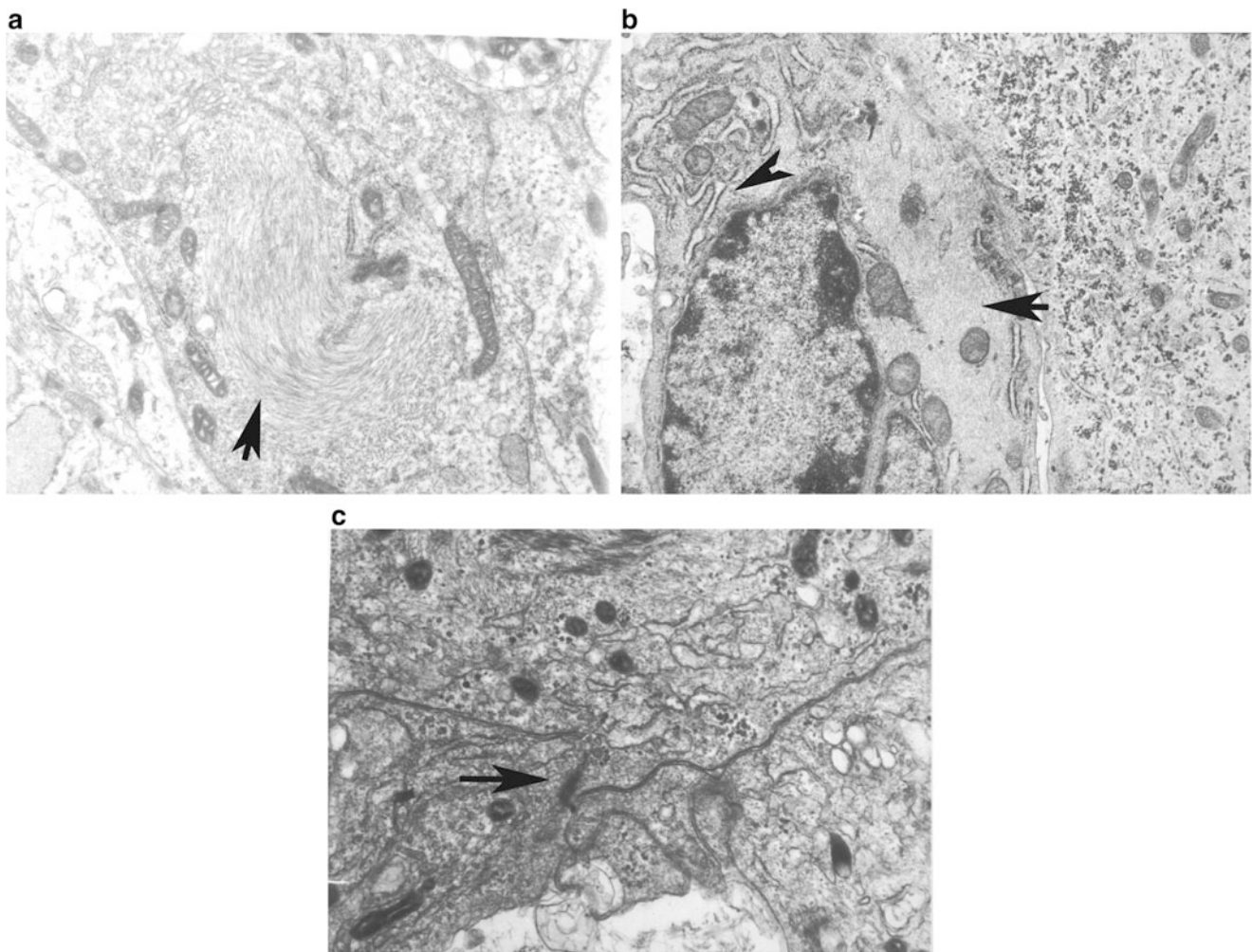
**Fig. 9.21** Ultrastructural features of AT/RT: (**A**) Large mass of intracytoplasmic whorls of intermediate filaments (*arrow*). (**B**) Intracytoplasmic filaments (*short arrow*) and dilated endoplasmic reticulum (*arrowhead*). (**C**) Prominent cell junctions (*arrow*)

- Gene expression studies have identified two subgroups of AT/RTs with differing genetic signatures:
  - Group 1 AT/RTs are predominantly supratentorial and are highly enriched for genes involved in brain or neural development and axonal guidance, with upregulation of NOTCH developmental signaling pathway genes including *FABP725* and *ASCL1*, which are markers of primitive neural lineage.
  - Group 2 AT/RTs are predominantly infratentorial and show enrichment of genes involved in mesenchymal differentiation and the bone morphogenetic protein (BMP) signaling pathway, including the *BMP4*, *BAMBI*, *SOST*, *SERPINF1*, *FBN2*, and *MSX1* loci. Mitogen-activated protein kinase (MAPK) signaling pathway genes and genes regulating cell adhesion and migration are also enriched in group 2 tumors.
- Expression of *ASCL* shows correlation with supratentorial location and superior 5-year overall survival.

- Integrated analyses of molecular subgroupings with clinical prognostic factors has demonstrated three distinct clinical risk groups of tumors with different therapeutic outcomes:
  - Localized supratentorial tumor with high *ASCL1* expression and complete surgical resection identifies a favorable risk category with a projected 5-year progression-free survival and overall survival of 60 %.
  - Metastatic or subtotally resected infratentorial tumor with no *ASCL1* expression represents the worst prognostic group, with greater than 80 % mortality within 24 months.
  - High-risk patients with *ASCL1*-positivity, localized but subtotally resected supratentorial or infratentorial tumors, have intermediate outcome and progression.
- CSF dissemination is a frequent terminal event (Fig. 9.22).
- Long-term survival has been observed in some patients with AT/RTs in the setting of rhabdoid predisposition syndrome (RPS).
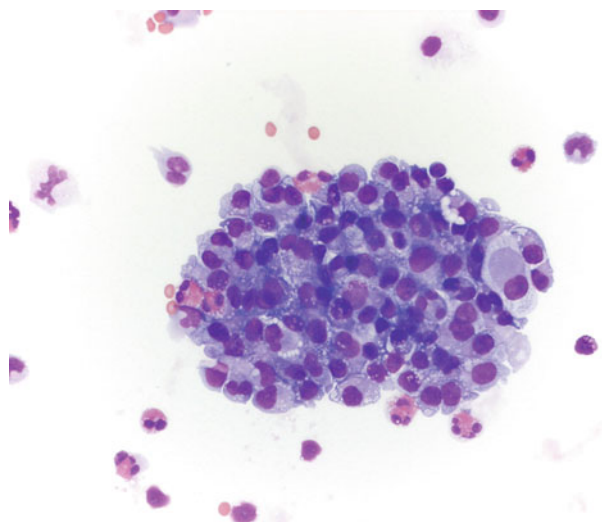
**Fig. 9.22** Cluster of malignant cells in the CSF in a patient with disseminated AT/RT

## Suggested Reading

Ammerlaan AC, Ararou A, Houben MP, Baas F, Tijssen CC, Teepen JL, et al. Long-term survival and transmission of INI1-mutation via nonpenetrant males in a family with rhabdoid tumour predisposition syndrome. Br J Cancer. 2008;98:474–9.

Burger PC, Yu IT, Tihan T, Friedman HS, Strother DR, Kepner JL, et al. Atypical teratoid/rhabdoid tumor of the central nervous system: a highly malignant tumor of infancy and childhood frequently mistaken for medulloblastoma: a Pediatric Oncology Group study. Am J Surg Pathol. 1998;22:1083–92.

Giangaspero F, Rigobello L, Badiali M, Loda M, Andrieini L, Basso G, et al. Large cell medulloblastomas. A distinct variant with highly aggressive behavior. Am J Surg Pathol. 1992;16:687–93.

Jackson EM, Shaikh TH, Gururangan S, Jones MC, Malkin D, Nikkel SM, et al. High-density single nucleotide polymorphism array analysis in patients with germline deletions of 22q11.2 and malignant rhabdoid tumor. Hum Genet. 2007;122:117–27.

Judkins AR, Mauger J, Rorke LB, Biegel JA. Immunohistochemical analysis of hSNF5/INI1 in pediatric CNS neoplasms. Am J Surg Pathol. 2004;28:644–50.

Judkins AR, Burger PC, Hamilton RL, Kleinschmidt-DeMasters B, Perry A, Pomeroy SL, et al. INI 1 protein expression distinguishes atypical teratoid/rhabdoid tumor from choroid plexus carcinoma. J Neuropathol Exp Neurol. 2005;64:391–7.

Louis DN, Perry A, Reifenberger G, von Deimling A, Figarella-Branger D, Cavenee WK, Ohgaki H, Wiestler OD, Kleihues P, Ellison DW. The 2016 World Health Organization classification of tumors of the central nervous system: a summary. Acta Neuropathol. 2016;131:803–20.

Louis DN, Ohgaki H, Wiestler OD, Cavenee WK, editors. WHO classification of tumours of the central nervous system. Lyon: International Agency for Research on Cancer (IARC); 2016.

Manhoff DT, Rorke LB, Yachnis AT. Primary intracranial atypical teratoid/rhabdoid tumor in a child with Canavan disease. Pediatr Neurosurg. 1995;22:214–22.

Meyers SP, Khademian ZP, Biegel JA, Chuang SH, Korones DN, Zimmerman RA. Primary intracranial atypical teratoid/rhabdoid tumors of infancy and childhood: MRI features and patient outcomes. AJNR Am J Neuroradiol. 2006;27:962–71.

Rorke LB, Packer RJ, Biegel JA. Central nervous system atypical teratoid/rhabdoid tumors of infancy and childhood: definition of an entity. J Neurosurg. 1996;85:56–65.

Sévenet N, Sheridan E, Amram D, Schneider P, Handgretinger R, Delattre O. Constitutional mutations of the hSNF5/INI1 gene predispose to a variety of cancers. Am J Hum Genet. 1999;65: 1342–8.

Torchia J, Picard D, Lafay-Cousin L, Hawkins CE, Kim SK, Letourneau L, et al. Molecular subgroups of atypical teratoid rhabdoid tumours in children: an integrated genomic and clinicopathological analysis. Lancet Oncol. 2015;16:569–82.